

# Effects of HE and ECAP processes on changes in microstructure and mechanical properties in copper, iron and zinc

Mariusz KULCZYK<sup>✉\*</sup>, Monika SKORUPSKA, Jacek SKIBA, Sylwia PRZYBYSZ,  
and Julita SMALC-KOZIOROWSKA

Institute of High Pressure Physics of the Polish Academy of Sciences UNIPRESS, Sokołowska 29/37, 01-142 Warsaw, Poland

**Abstract.** The research presented in this paper concerns the influence of the rate of plastic deformation generated directly in the processes of severe plastic deformations on the microstructure and properties of three metals: copper, iron and zinc. The equal channel angular pressing (ECAP) method was used, and it was performed at a low plastic deformation rate of  $\sim 0.04 \text{ s}^{-1}$ . The high plastic strain rate was obtained using the hydrostatic extrusion (HE) method with the deformation rate at the level of  $\sim 170 \text{ s}^{-1}$ . For all three tested materials different characteristic effects were demonstrated at the applied deformation rates. The smallest differences in the mechanical properties were observed in copper, despite the dynamic recrystallization processes that occurred in the HE process. In Armco iron samples, dynamic recovery processes in the range of high plastic deformation rates resulted in lower mechanical properties. The most significant effects were obtained for pure zinc, where, regardless of the method used, the microstructure was clearly transformed into bimodal after the ECAP process, and homogenized and refined after the HE process. After the HE process, the material was transformed from a brittle state to a plastic state and the highest mechanical properties were obtained.

**Key words:** hydrostatic extrusion; equal channel angular pressing; rate of plastic deformation; copper; iron; zinc.

## 1. INTRODUCTION

In previous international publications on the influence of high rates of plastic deformation on the properties of metals, the characteristics of static or dynamic hardening of materials that occur during single-axis tensile tests and by using the “Split-Hopkinson pressure bar” [1] or the “Pendulum-driven tensile Kolsky bar” [2], are strictly research processes which are not plastic forming processes. In this paper, a wide range of plastic strain rates will be generated in the processes of severe plastic deformations (SPD), i.e. equal channel angular pressing (ECAP) and hydrostatic extrusion (HE), which are used to produce materials with unique mechanical properties by refining the microstructure to the ultra-fine-grained or nanocrystalline level. The ECAP process is one of the most popular methods of severe plastic deformation, used by many research centers to analyze changes in the properties of a wide range of materials, mainly metals and metal alloys [3–6]. The ECAP process is usually carried out at relatively low strain rates, from  $\sim 10^{-2} \text{ s}^{-1}$  up to  $\sim 10^{-1} \text{ s}^{-1}$  [7–9]. Hydrostatic extrusion is a method of introducing severe plastic deformations, unique on a global scale, and the Institute of High Pressure Physics of the Polish Academy of Sciences is a leading research unit developing this technology. Its efficiency, which is related to the refinement of the material microstructure, has been repeatedly

presented in scientific publications, both for the materials susceptible to plastic deformations, such as aluminum, aluminum alloys, copper alloys and hard-deformable materials, such as steel or titanium, and even plastics [10–17]. One of the characteristic features of the HE process is its high strain rate, reaching  $\sim 10^4 \text{ s}^{-1}$ , which is over four orders of magnitude higher compared to the ECAP method [18]. The paper contains a comparison of the ECAP and HE methods, performed at extreme strain rates at the level of  $\sim 10^{-2} \text{ s}^{-1}$  for ECAP and  $\sim 10^3 \text{ s}^{-1}$  for HE, respectively. Such kind of research has not been carried out so far, and the ECAP method in conjunction with the HE process was used only to intensify the effect of strain hardening after complex plastic forming processes. The complex plastic forming processes ECAP and HE were carried out using such materials as pure nickel, aluminum, copper or 5xxx series aluminum alloys [10, 19–21]. In all cases, when the combination of ECAP+HE was applied, a significant increase in mechanical properties and microstructure homogenization were observed. In the scope of the research, ECAP and HE processes were carried out with the use of three materials, i.e. pure copper, Armco iron and zinc. Face-Centred Cubic (FCC) copper has a crystal structure and is susceptible to plastic deformation with high reduction rates [20]. Body-Centered Cubic (BCC) steel tends to significantly increase its strength. Earlier research showed a tensile strength increase of ARMCO iron to the level of UTS  $\sim 1500 \text{ MPa}$  after the process of extrusion with the total actual strain  $\varepsilon = 6.5$  [22]. Zinc has a hexagonal close-packed crystal structure (HCP). It is easily subjected to plastic formation processes and what is worth noting it recrystallizes at room tem-

\*e-mail: [mariusz@unipress.waw.pl](mailto:mariusz@unipress.waw.pl)

Manuscript submitted 2022-08-26, revised 2023-01-30, initially accepted for publication 2023-02-27, published in June 2023.

perature [23]. The conventional basic testing procedure, which is the single-axis static stretching, was used only to study the effects related to the influence of the rate of strain that occurred during plastic deformation on the final mechanical properties of selected materials. Changes in the rate of deformation during severe plastic deformation processes, in contrast to the changes in later mechanical tests, enabled us to carry out microstructural observations, and not only to examine fractures. The aforementioned research processes utilizing methods such as the 'Pendulum-driven tensile Kolsky bar' and comparing static and dynamic stains were carried out for titanium, among others [2]. Elongation in dynamic tests was lower by 50%. The phenomenon was accompanied by an increase in the strain hardening in the entire range of the strain rates tested (starting from the yield point  $Y_S = 350$  MPa in the static test, to  $Y_S = 575$  MPa for the strain rate of  $1.1 \times 10^3$  s<sup>-1</sup> in dynamic tests. In the future, the determination of changes in mechanical and microstructural properties of materials depending on the strain rate and the method of deformation will facilitate optimizing plastic working processes in terms of their final requested properties.

## 2. MATERIALS AND EXPERIMENTS

Three materials were tested: copper with a purity of 99.9%, Armco iron with a purity of 99.7% and zinc with a purity of 99.9%. In order to homogenize the microstructure, iron and zinc were annealed. Armco iron bar was vacuum annealed at 930°C for one hour and then cooled inside the furnace to ambient temperature. The zinc bar was annealed at 150°C for 30 minutes. Samples for the ECAP process with a square cross-section of 10 × 10 mm and a length of 60 mm were machined out of all the tested bars with a diameter of 30 mm. All materials were subjected to two steps ECAP process at room temperature using a die with a 90° angle between the channels and route C, in which the sample was turned 180° around its axis between passes. ECAP was performed to give a strain rate of 0.04 s<sup>-1</sup>. The ECAP specimens were made with a cumulative true strain  $\epsilon \sim 2$ . All materials in the form of a rod with a diameter of 16 mm were subjected to a single hydrostatic extrusion process with a true strain the same as for the ECAP process, i.e.,  $\epsilon \sim 2$  for the final diameter of 6 mm.

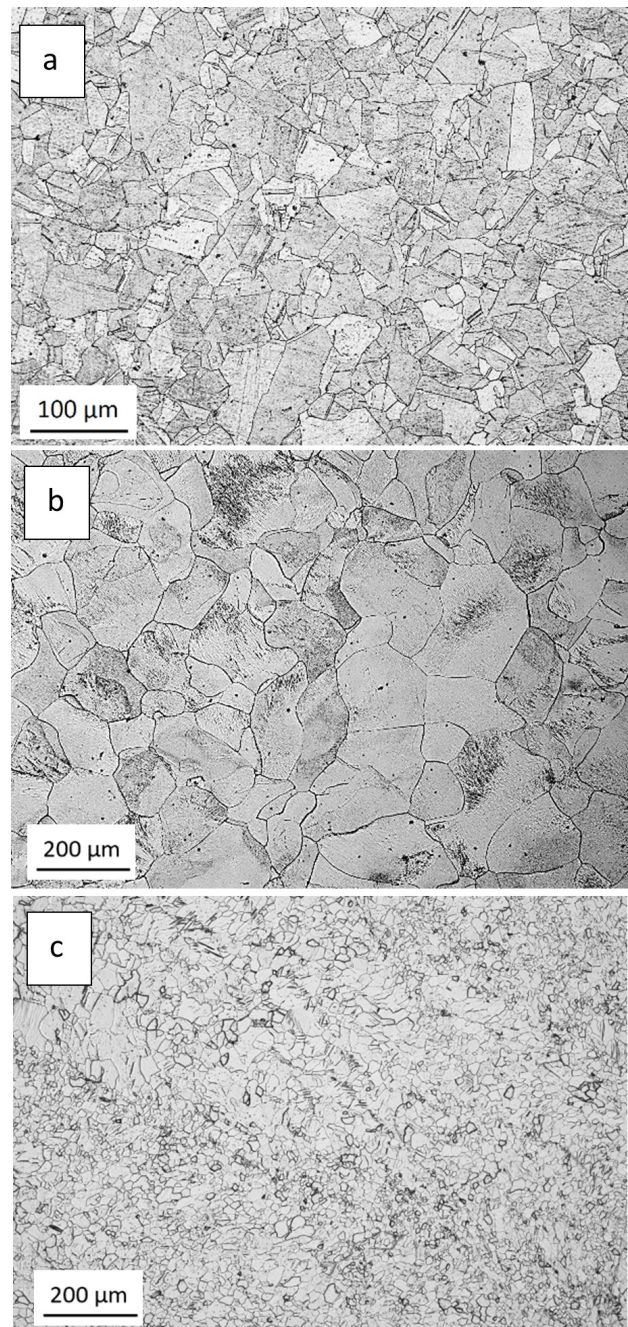
Starting from a distance of about 10 cm from the die exit, the outgoing deformed materials were intensively cooled using running water. The HE processes were carried out with a plastic deformation speed of 170 s<sup>-1</sup>. The rate of plastic strain was controlled by the volume of the pressure medium and the speed of its compression. Hydrostatic extrusion was conducted through a die with an apex angle of  $2\alpha = 45^\circ$ . A detailed characterization of the hydrostatic extrusion process was presented in previous publications [14, 18]. Samples for microstructural studies from initial materials and after plastic strain were prepared from transverse cross-sections. Microscopic observations were carried out using a Nikon Eclipse LV150 optical microscope and the FEI TECNAI G2 F20 transmission electron microscope. The microstructure in terms of the grain size before and after the HE and ECAP processes was quantitatively evaluated using the 'Micrometer' software [24]. The grain size was

determined by measuring the equivalent diameter ( $d_2$ ) defined as the diameter of the circle with a surface area equal to that of a given grain. The tensile properties were investigated in a Zwick/Roell Z250kN static tensile machine with a constant strain rate of 0.008 s<sup>-1</sup> and length-to-diameter ratio = 5.

## 3. RESULTS AND DISCUSSION

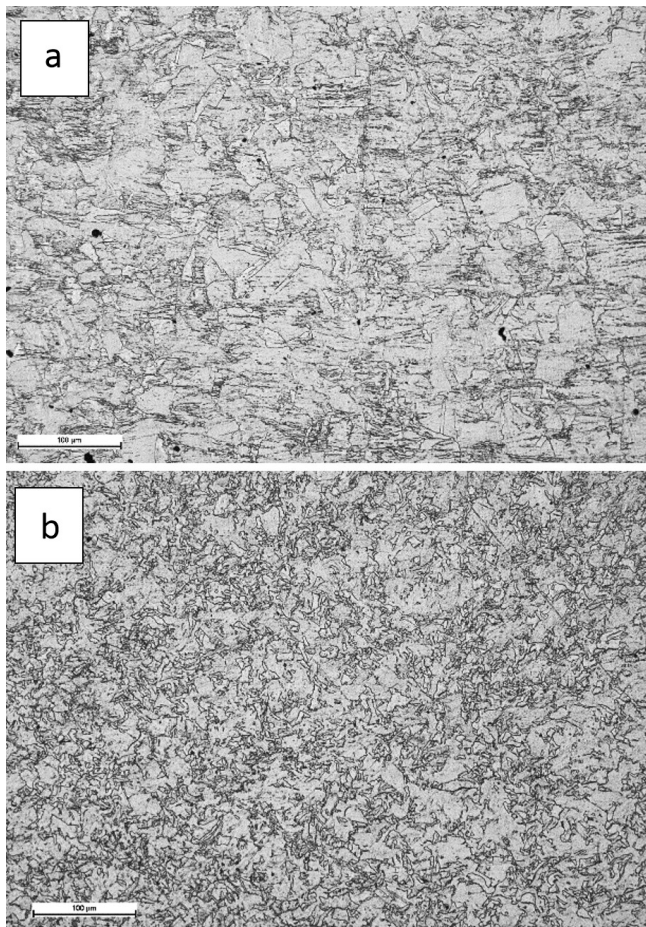
### 3.1. Microstructure

Figure 1 shows the microstructure of copper, iron and zinc in the initial state, before plastic deformation processes, after heat treatment processes.



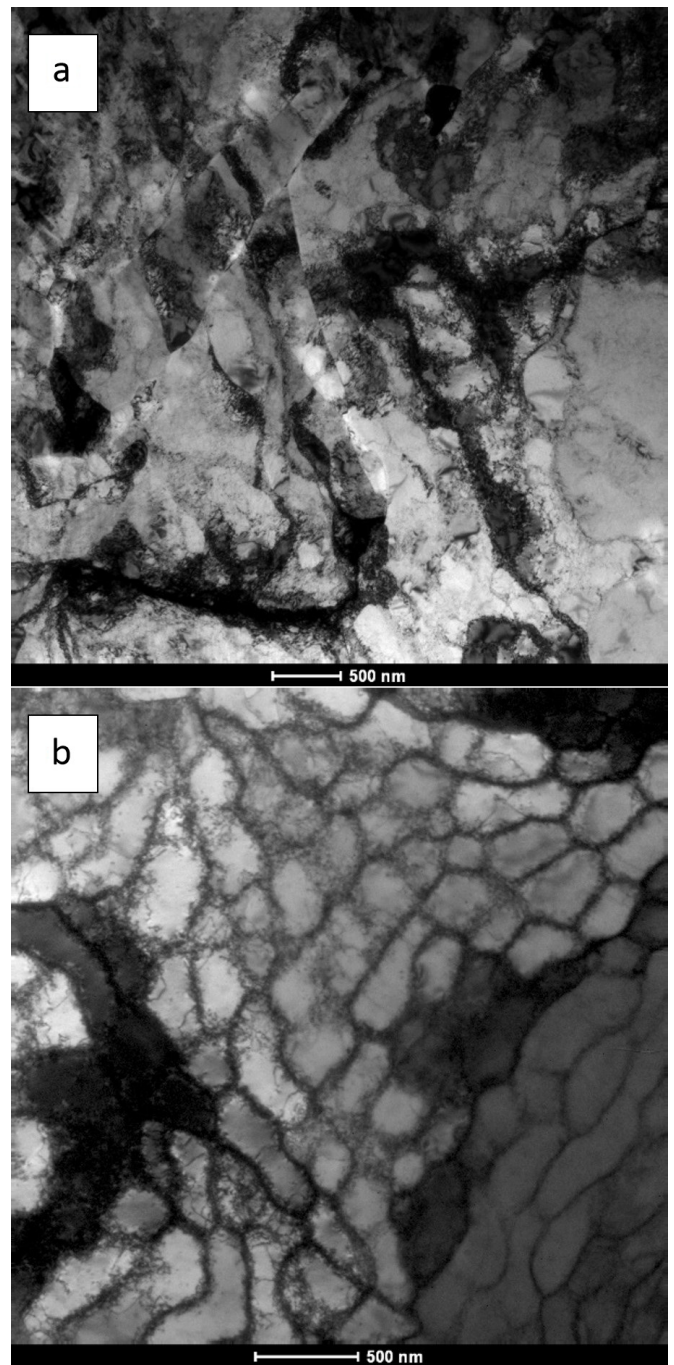
**Fig. 1.** Microstructure of the tested materials in the initial state: (a) copper; (b) Armco iron; (c) zinc

All three tested materials, before the plastic deformation, had homogeneous microstructures of equiaxed grains. The average grain size was  $d_2 \sim 45 \mu\text{m}$  for copper,  $d_2 \sim 98 \mu\text{m}$  for iron and  $d_2 \sim 15 \mu\text{m}$  for zinc. Figure 2 presents images of the copper microstructure after the ECAP process with a strain rate of  $0.04 \text{ s}^{-1}$  and after the HE process with a strain rate of  $170 \text{ s}^{-1}$ . In the images obtained with a light microscope after the ECAP process, the boundaries of the primary grains and the distorted and deformed grains are visible in Fig. 2a. These boundaries are not visible in samples after the HE process, and the microstructure looks much more defected, see Fig. 2b.



**Fig. 2.** Copper microstructure after the ECAP process (a) and after the HE process; (b) with the total real strain  $\epsilon \sim 2$

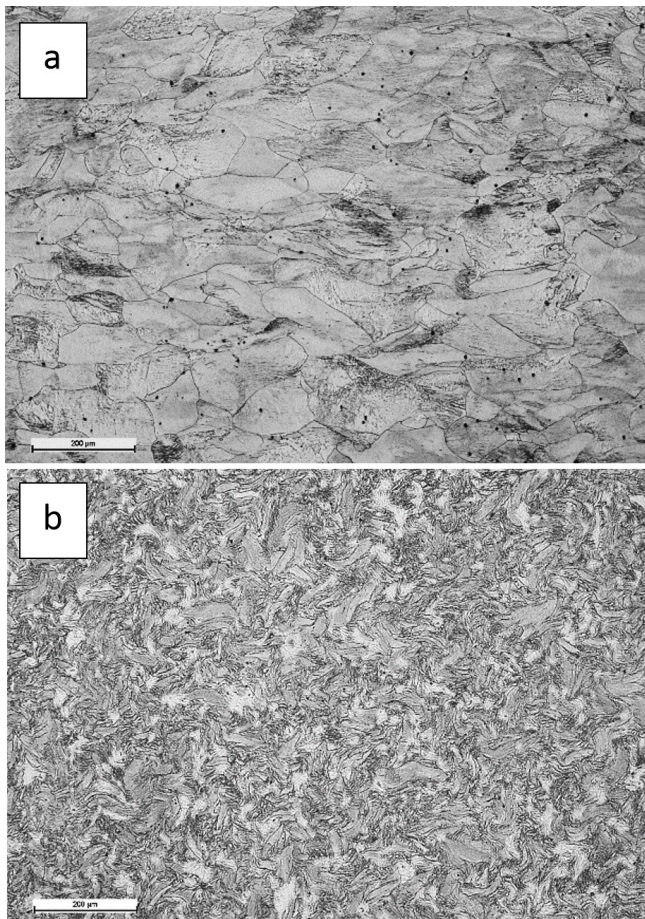
Figure 3 shows the microstructure of copper after plastic deformation, obtained using the transmission electron microscopy technique. After the ECAP process, clear primary grain boundaries strongly defective inside were observed, see Fig. 3a. The microstructure of copper after the HE process is significantly different. Cellular dislocation structures and subgrains with an average size of  $d_2 \sim 200 \text{ nm}$  are visible, see Fig. 3b. The phenomenon is related to a strong thermal effect occurring at high strain rates, leading to dynamic recrystallization processes in the strain zone. The static recrystallization processes are eliminated by a strong cooling of the material after exiting the matrix in the HE process. As demonstrated in previous



**Fig. 3.** The TEM microstructure of copper after the ECAP (a) process and the HE; (b) process with total real strain  $\epsilon \sim 2$

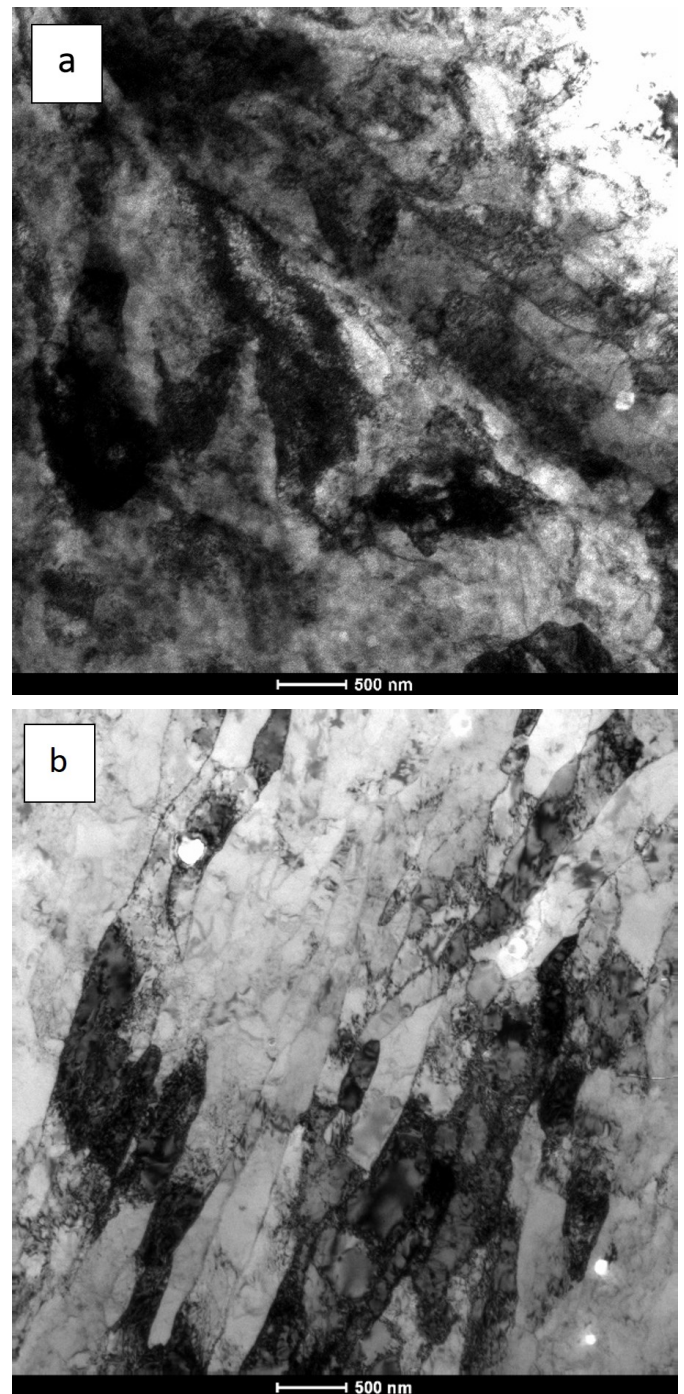
studies, such plastic deformation conditions generate a temperature of  $250\text{--}300^\circ\text{C}$ , which is high enough for the recrystallization processes to occur [25]. The same work presents the microstructure of pure copper after the HE process with 50% lower deformation, i.e.  $\epsilon \sim 1$ , showing a similar character as after the ECAP process, where the primary grain boundaries were visible. This proves that initiating the copper structure defects is more effective under the conditions of a much higher rate of plastic deformation that accompanies the HE process.

Figure 4 shows the iron microstructure after the ECAP and HE processes, in both cases at the actual rate of  $\epsilon \sim 2$ . As in the case of copper, defected primary grains are observed after the ECAP process in Armco iron, Fig. 4a. After the HE process, the microstructure is severely deformed and the primary grains are not visible. In TEM images captured after the ECAP process, clear primary grain boundaries severely defective inside were visible, as shown in Fig. 5a. After the HE process, the microstructure had visible strips, see Fig. 5b. The thin deformation strips (about 100–200 nm wide) have low disorientation angles as evidenced by a single orientation visible in the diffraction image. Many of the observed strips are free of internal defects, which may indicate the dynamic healing processes taking place in the extruded iron under high-pressure conditions and at a high rate of plastic deformation, four orders of magnitude greater than in the ECAP process.



**Fig. 4.** Armco iron microstructure after the ECAP process (a) and the HE process; (b) with the total actual strain  $\epsilon \sim 2$

The static recovery processes in severely deformed Armco iron were previously presented for the same material after the 16 x ECAP process [26]. This process occurred during the post-deformation heat treatment at the temperature of  $\sim 350^\circ\text{C}$ . Such a temperature range is accompanied by plastic deformation in the strain zone during the HE process, which favors this process in a dynamic form.



**Fig. 5.** a) Armco iron TEM microstructure after the ECAP process with the total actual strain  $\epsilon \sim 2$ ; b) Armco iron TEM microstructure after the HE process with the total actual strain  $\epsilon \sim 2$

Figure 6 shows the zinc microstructure after the ECAP and HE processes, in both cases with the total actual strain  $\epsilon \sim 2$ . After the ECAP process, a bimodal microstructure was observed, Fig. 6a. The average grain size  $d_2 \sim 6 \mu\text{m}$  with the coefficient of the grain size distribution variation  $Cv_{d_2} = 1.05$ .

In the initial state, before the plastic deformation process, the calculated value of the Cv coefficient  $d_2$  was 0.5. After the ECAP process, the fraction of smaller grains was ob-

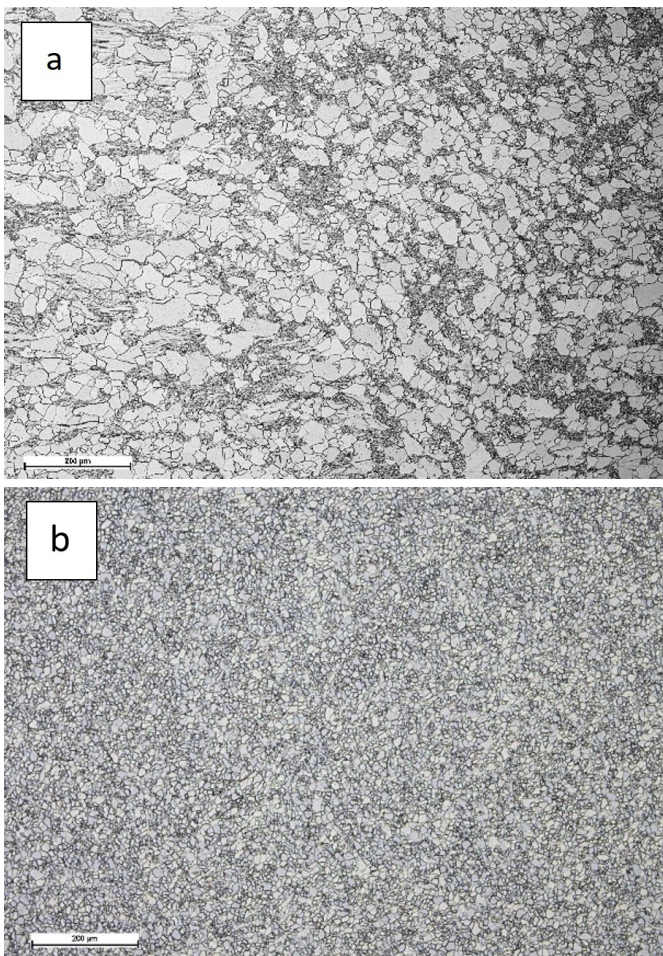


**Fig. 6.** Zinc microstructure after the ECAP process (a) and after the HE process; (b) with the total real strain  $\varepsilon \sim 2$

served within the range of  $d_2 = 5\text{--}10\ \mu\text{m}$  and the fraction of larger grains within the range of  $d_2 = 15\text{--}30\ \mu\text{m}$ . After the HE process, the microstructure is made of homogeneous, even-axis grains with an average size of  $d_2 = 5.5\ \mu\text{m}$ . The variation in particle size distribution coefficient was  $C_{vd_2} = 0.4$ , which proves greater homogeneity of the microstructure than in the initial state before the plastic deformation process. Clear grains after the HE process are visible in the image of the microstructure obtained using the TEM technique, see Fig. 7b. No defects inside the grains indicate the processes of intensive dynamic recrystallization during the plastic deformation process. This is favored by the susceptibility of zinc to recrystallization processes, which can take place in this material at room temperature. Similar nature of microstructural changes was observed in zinc subjected to cold compression processes with a degree of compression of 161%, where, after exceeding the strain rate of  $0.5\ \text{s}^{-1}$ , a homogeneous microstructure was observed with an average grain size of  $d_2 = 24\ \mu\text{m}$  [27]. These changes were attributed to the process of continuous dynamic recrystallization that occurred at a sufficiently high degree of material compaction and a sufficiently high rate of strain.

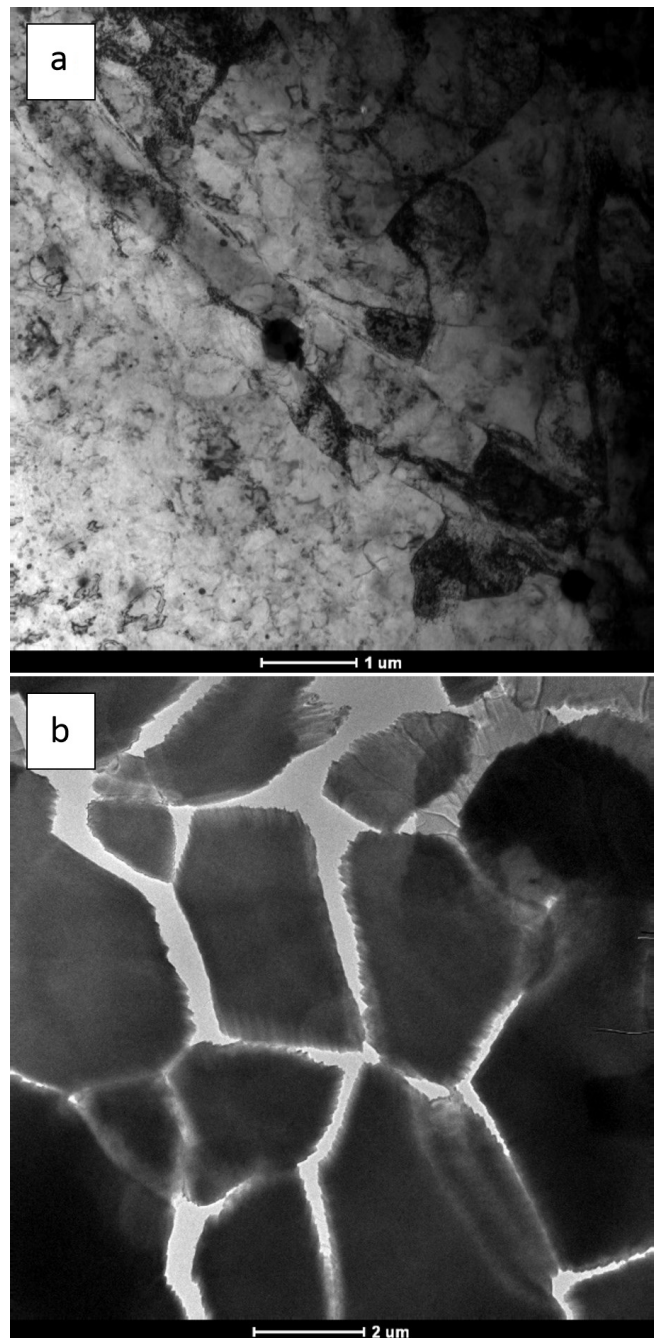


**Fig. 7.** Zinc microstructure after the ECAP process (a) and after the HE process; (b) with the actual total strain  $\varepsilon \sim 2$

### 3.2. Mechanical properties

Figure 8 shows the stress-strain curves for copper deformed at the minimum rate using the ECAP method, i.e.  $0.04\ \text{s}^{-1}$  and the maximum rate using the HE method –  $170\ \text{s}^{-1}$  and a comparison of the obtained mechanical properties to the properties of the material in the initial state, see Fig. 8b. The increase in mechanical properties, regardless of speed, in both cases is significant and amounts to nearly 50% for YS and UTS compared to the starting material. Comparing the ECAP and HE methods, it is worth noting that after the HE process, the ob-

tained strength values, both YS and UTS, are slightly higher (about 5%) with the elongation value lower by ~ 1%. The maximum values of ultimate tensile strength and yield strength are UTS = 427 MPa and YS = 425 MPa, respectively. With regard to the microstructural analysis presented earlier, where a significantly different nature of changes in the copper microstructure after both processes was shown, it seems interesting to obtain similar mechanical properties for both materials. This effect may be related to the specificity of both processes. The slow rate of deformation accompanying the ECAP process initiates the generation of structural defects and slow hardening of the material during plastic deformation. Very high rates of plastic deformation in the HE process lead to a very effective generation of defects, which is additionally accompanied by strong thermal effects eliminating the effects of strengthening in dynamic recrystallization processes. As a result, a different character of the microstructure after both processes is obtained but mechanical properties are similar.

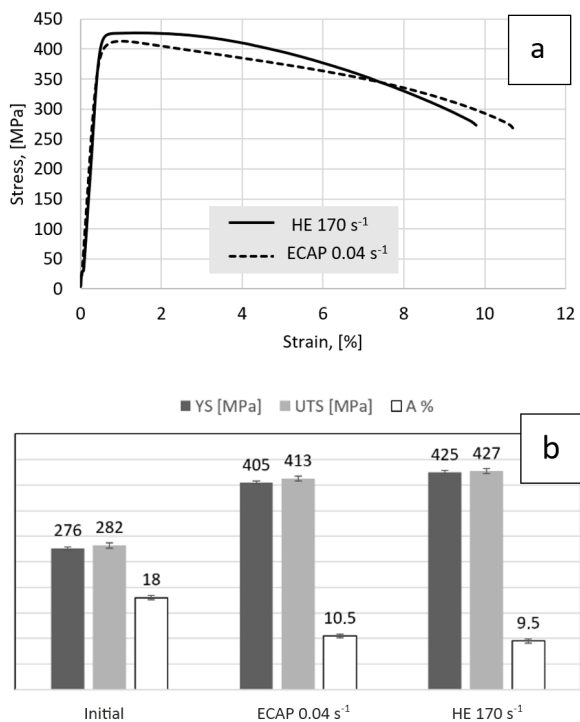


**Fig. 8.** Mechanical properties of copper after plastic deformation using the ECAP and HE methods, tensile curves (a); comparison to the material in the initial state (b)

Different nature of changes in mechanical properties was observed in the Armco iron. Figure 9 shows the stress-strain curves for Armco iron deformed using the ECAP and HE methods, together with a comparison of the obtained mechanical properties in relation to the material in its initial state, see Fig. 9b. After the hydrostatic extrusion process, at very high plastic deformation rates, the obtained mechanical properties are significantly lower compared to the properties after the ECAP process. The differences between the obtained values of ultimate tensile strength and yield strength in the ECAP and HE

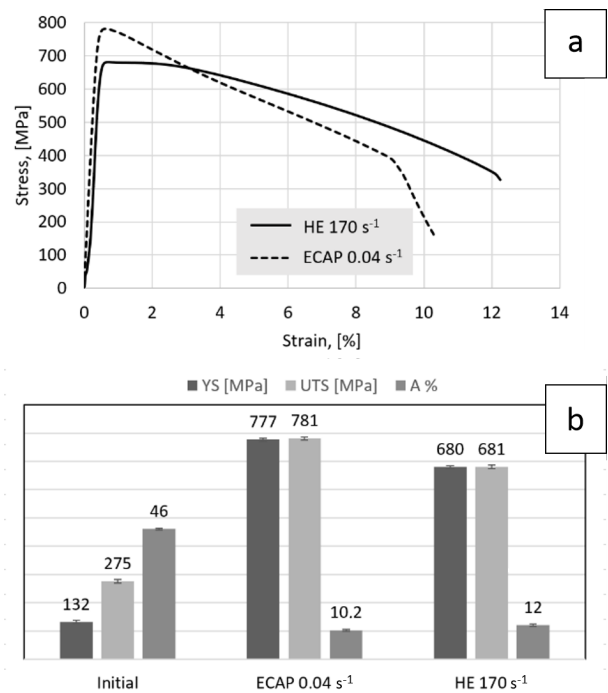


**Fig. 9.** Mechanical properties of Armco after plastic deformation using the ECAP and HE methods, tensile curves (a); comparison to the material in the initial state (b)

processes are ~ 15%. The maximum values of yield strength and ultimate tensile strength obtained in the ECAP process are YS = 781 MPa and UTS = 777 MPa, respectively, with an elongation of ~ 10%, which is slightly lower compared to the HE process. As presented in the description of the Armco iron microstructure, the intensity of plastic deformation promotes the recovery processes, in this case in a dynamic form, and its effects under conditions of high plastic deformation rates are related to the mechanical properties obtained in the HE process. Nevertheless, it is worth noting that, in comparison to the material in the initial state, both plastic deformation processes, i.e. ECAP and HE, show a clear increase in mechanical properties, accompanied by an increase in yield strength YS by nearly 500%. This results in a distinct reduction in elongation compared to the initial value of 46%. However, in both cases, the material is still ductile and the elongation exceeds 10%. The strongest effects of deformation rate in the ECAP and HE methods were observed for pure zinc. Figure 10 shows the stress-strain curves for zinc deformed at the minimum rate using the ECAP method, i.e. 0.04 s<sup>-1</sup> and the maximum rate using the HE method – 170 s<sup>-1</sup> and a comparison of the obtained mechanical properties to the properties of the material in the initial state, see Fig. 10b. The material in the initial state is brittle and its elongation is only 2%. After the ECAP process with a low deformation rate, despite a significant increase in mechanical properties, the elongation does not improve and the obtained value is still 2%. After the hydrostatic extrusion process, a rapid increase in elongation value to the level of nearly 50% is observed. This is accompanied by the highest obtained values of yield strength YS = 145 MPa and ultimate

tensile strength UTS = 194 MPa (the increase compared to the material in the initial state values  $\sim 380\%$  and  $\sim 220\%$ , respectively). The obtained effects of changes in mechanical properties reflect the microstructural studies presented earlier in this paper. The bimodal microstructure obtained in the ECAP process at low deformation rates increases the mechanical properties but does not improve the plasticity of the material. High homogenization and refinement of the microstructure in the HE process at high deformation rates, accompanied by strong dynamic recrystallization processes, improve the plasticity of the material with a significant increase in mechanical properties.

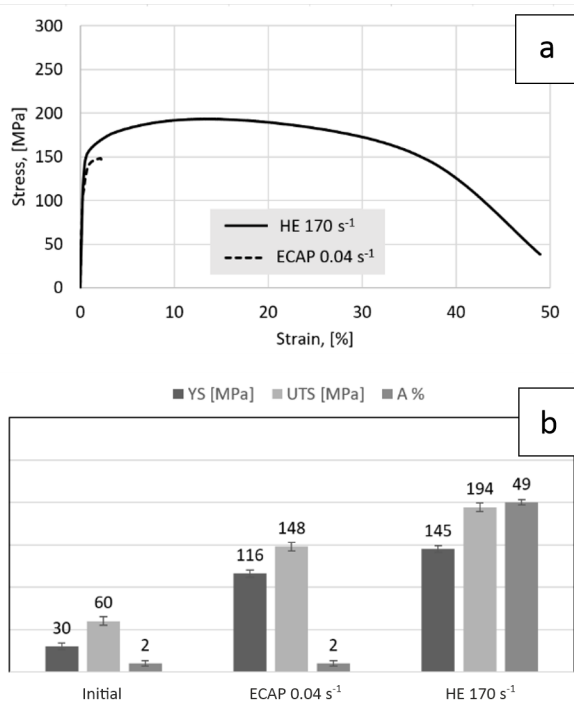


**Fig. 10.** Mechanical properties of zinc after plastic deformation using the ECAP and HE methods, tensile curves (a); comparison to the material in the initial state (b)

#### 4. CONCLUSIONS

The study attempts to compare the influence of extreme plastic deformation rates, i.e.  $0.04 \text{ s}^{-1}$  in the ECAP process and  $170 \text{ s}^{-1}$  in the HE process on changes observed in the microstructure and mechanical properties of three pure metals: copper, Armco iron and zinc. For all the tested materials and characteristics different effects of the strain rate were obtained:

- for copper, despite the clear differences in the microstructure related to the formation of the sub-grain structure in the processes of dynamic recrystallization accompanying the high rate of plastic deformation when using the HE method, no clear difference in the obtained mechanical properties was observed. The yield strength and ultimate tensile strength were about 5% higher after the HE process,
- for Armco iron, after plastic deformation with high strain rates using the HE process, clear dynamic healing effects were observed, which resulted in the weakening of the pro-

cess of strengthening and obtaining significantly lower mechanical properties compared to properties achieved by using the ECAP method. Nevertheless, both processes caused strong strengthening, increasing the value of the yield strength by  $\sim 500\%$ , up to the maximum value of YS = 777 MPa (the ECAP process),

- for zinc, both strain rates were accompanied by a complete transformation of microstructure. Slow deformation in the ECAP process resulted in the formation of a bimodal grain microstructure ( $d_2 \sim 6 \mu\text{m}$ ) with a clear hardening of the material, but increased brittleness. Rapid deformation in the HE process caused by the phenomenon of dynamic recrystallization resulted in refinement ( $d_2 \sim 5.5 \mu\text{m}$ ) and a strong homogenization of the microstructure. The result was a significant improvement in the plasticity of the material with the highest mechanical properties.

The different natures of microstructural changes and mechanical properties in all tested materials, depending on the plastic deformation rates and the method used, indicate how important it is to select and optimize plastic working parameters in order to obtain the desired properties of the materials.

#### ACKNOWLEDGEMENTS

This work was carried out within the OPUS 13 Project financed by the National Science Centre – Poland under project no. 2017/25/B/ST8/01118.

#### REFERENCES

- [1] A.K. Ghosh, “The Influence of Strain Hardening and Strain-Rate Sensitivity on Sheet Metal Forming,” *J. Eng. Mater. Technol.*, vol. 99, no. 3, pp. 264–274, 1977, doi: [10.1115/1.3443530](https://doi.org/10.1115/1.3443530).
- [2] J.M. Yuan and V.P.W. Shim, “Tensile response of ductile  $\alpha$ -titanium at moderately high strain rates,” *Int. J. Solids Struct.*, vol. 39, no. 1, pp. 213–224, 2002, doi: [10.1016/S0020-7683\(01\)00214-1](https://doi.org/10.1016/S0020-7683(01)00214-1).
- [3] V.M. Segal, “Materials processing by simple shear,” *Mater. Sci. Eng. A*, vol. 197, no. 2, pp. 157–164, 1995, doi: [10.1016/0921-5093\(95\)09705-8](https://doi.org/10.1016/0921-5093(95)09705-8).
- [4] T. Tański, P. Snopiński, and W. Borek, “Strength and structure of AlMg3 alloy after ECAP and post-ECAP processing,” *Mater. Manuf. Process.*, vol. 32, no. 12, pp. 1368–1374, 2017, doi: [10.1080/10426914.2016.1257131](https://doi.org/10.1080/10426914.2016.1257131).
- [5] H. Jia and Y. Li, “Texture evolution of an Al-8Zn alloy during ECAP and post-ECAP isothermal annealing,” *Mater. Charact.*, vol. 155, p. 109794, 2019, doi: [10.1016/j.matchar.2019.109794](https://doi.org/10.1016/j.matchar.2019.109794).
- [6] G.I. Raab, I.S. Kodirov, D.A. Aksenova, and R.Z. Valiev, “The formation of a high-strength state in martensitic Ti Grade 4 by ECAP,” *J. Alloy. Compd.*, vol. 922, p. 166205, 2022, doi: [10.1016/j.jallcom.2022.166205](https://doi.org/10.1016/j.jallcom.2022.166205).
- [7] K.V. Ivanov and E.V. Naidenkin, “Effect of the Velocity of Equal-Channel Angular Pressing on the Formation of the Structure of Pure Aluminum,” *Phys. Metals Metallogr.*, vol. 106, no. 4, pp. 411–417, 2008, doi: [10.1134/S0031918X08100116](https://doi.org/10.1134/S0031918X08100116).
- [8] S.E. Mousavi, M.H. Khaleghifar, M. Meratian, B. Sadeghi, and P. Cavaliere, “Effect of the equal channel angular pressing route on the microstructural and mechanical behavior of Al-5086 alloy,” *Materialia*, vol. 4, pp. 310–322, 2018, doi: [10.1016/j.mtla.2018.10.007](https://doi.org/10.1016/j.mtla.2018.10.007).

- [9] P.B. Berbon, M. Furukawa, Z. Horita, M. Nemoto, and T.G. Langdon, "Influence of pressing speed on microstructural development in equal-channel angular pressing," *Metall. Mater. Trans. A*, vol. 30, pp. 1989–1997, 1999, doi: [10.1007/s11661-999-0009-9](https://doi.org/10.1007/s11661-999-0009-9).
- [10] L. Olejnik, M. Kulczyk, W. Pachla, and A. Rosochowski, "Hydrostatic extrusion of UFG aluminium," *Int. J. Mater. Form.*, vol. 2, no. 1, pp. 621–624, 2009, doi: [10.1007/s12289-009-0508-7](https://doi.org/10.1007/s12289-009-0508-7).
- [11] M. Orłowska *et al.*, "The Influence of Heat Treatment on the Mechanical Properties and Corrosion Resistance of the Ultrafine-Grained AA7075 Obtained by Hydrostatic Extrusion," *Materials*, 15, no. 12, p. 4343, 2022, doi: [10.3390/ma15124343](https://doi.org/10.3390/ma15124343).
- [12] S. Przybysz *et al.*, "Anisotropy of mechanical and structural properties in the AA 6060 aluminium alloy after the hydrostatic extrusion process," *Bull. Pol. Acad. Sci. Tech. Sci.*, vol. 67, no. 4, pp. 709–717, 2019, doi: [10.24425/bpasts.2019.130180](https://doi.org/10.24425/bpasts.2019.130180).
- [13] M. Kulczyk, J. Skiba, W. Pachla, J. Smalc-Koziorowska, S. Przybysz, and M. Przybysz, "The effect of high-pressure plastic forming on the structure and strength of AA5083 and AA5754 alloys intended for fasteners," *Bull. Pol. Acad. Sci. Tech. Sci.*, vol. 68, no. 4, pp. 903–911, 2020, doi: [10.24425/bpasts.2020.134183](https://doi.org/10.24425/bpasts.2020.134183).
- [14] M. Kulczyk *et al.*, "Improved compromise between the electrical conductivity and hardness of the thermo-mechanically treated CuCrZr alloy," *Mater. Sci. Eng. A*, 724, pp. 45–52, 2018, doi: [10.1016/j.msea.2018.03.004](https://doi.org/10.1016/j.msea.2018.03.004).
- [15] B. Skowrońska, T. Chmielewski, M. Kulczyk, J. Skiba, and S. Przybysz, "Microstructural Investigation of a Friction-Welded 316L Stainless Steel with Ultrafine-Grained Structure Obtained by Hydrostatic Extrusion," *Materials*, vol. 14, no. 6, p. 1537, 2021, doi: [10.3390/ma14061537](https://doi.org/10.3390/ma14061537).
- [16] Ł. Maj *et al.*, "Titania coating formation on hydrostatically extruded pure titanium by micro-arc oxidation method," *J. Mater. Sci. Technol.*, vol. 111, pp. 224–235, 2022, doi: [10.1016/j.jmst.2021.09.019](https://doi.org/10.1016/j.jmst.2021.09.019).
- [17] M. Skorupska, M. Kulczyk, S. Przybysz, J. Skiba, J. Mizeracki, and J. Ryszkowska, "Mechanical Reinforcement of Polyamide 6 by Cold Hydrostatic Extrusion," *Materials*, 14, no. 20, p. 6045, 2021, doi: [10.3390/ma14206045](https://doi.org/10.3390/ma14206045).
- [18] W. Pachla, J. Skiba, M. Kulczyk, and M. Przybysz, "Aparatura wysokociśnieniowa do przeróbki plastycznej materiałów z dużymi odkształceniami na zimno," High-pressure equipment for cold severe plastic deformation working of materials, *Obróbka Plastyczna Metali*, vol. XXVI, no. 4, pp. 283–306, 2015, ISBN: 0867-2628. (in Polish)
- [19] M. Kulczyk *et al.*, "Combination of ECAP and hydrostatic extrusion for UFG microstructure generation in nickel," *Solid State Phenomena*, vol. 114, pp. 51–56, 2006, doi: [10.4028/www.scientific.net/SSP.114.51](https://doi.org/10.4028/www.scientific.net/SSP.114.51).
- [20] M. Kulczyk, W. Pachla, A. Mazur, M. Suś-Ryszkowska, N. Krasilnikov, and K.J. Kurzydłowski, "Producing bulk nanocrystalline materials by combined hydrostatic extrusion and equal-channel angular pressing," *Mater. Sci.-Pol.*, vol. 25, no. 4, pp. 991–999, 2007.
- [21] M. Kulczyk, J. Skiba, and W. Pachla, "Microstructure and mechanical properties of AA5483 treated by a combination of ECAP and hydrostatic extrusion," *Arch. Metall. Mater.*, vol. 59, pp. 163–166, 2014, doi: [10.2478/amm-2014-0026](https://doi.org/10.2478/amm-2014-0026).
- [22] M. Kulczyk, W. Pachla, A. Świdorska-Środa, M. Suś-Ryszkowska, A. Mazur, and K.J. Kurzydłowski, "Nano- and Ultra-fine-grained Structures in Iron and Nickel induced by Hydrostatic Extrusion," *Proc. of The 9th International ESAFORM Conference on Material Forming*, UK, 2006.
- [23] A. Jarzębska *et al.*, "A new approach to plastic deformation of biodegradable zinc alloy with magnesium and its effect on microstructure and mechanical properties," *Mater. Lett.*, vol. 211, pp. 58–61, 2018, doi: [10.1016/j.matlet.2017.09.090](https://doi.org/10.1016/j.matlet.2017.09.090).
- [24] T. Wejrzanowski, W.L. Szychalski, K. Różniatowski, and K.J. Kurzydłowski, "Image based analysis of complex microstructures of engineering materials," *Int. J. Appl. Math. Comput. Sci.*, vol. 18, no. 1, pp. 33–39, 2008, doi: [10.2478/v10006-008-0003-1](https://doi.org/10.2478/v10006-008-0003-1).
- [25] W. Pachla *et al.*, "Enhanced strength and toughness in ultra-fine grained 99.9% copper obtained by cryo-hydrostatic extrusion," *Mater. Charact.*, vol. 141, pp. 375–387, 2018, doi: [10.1016/j.matchar.2018.04.048](https://doi.org/10.1016/j.matchar.2018.04.048).
- [26] J.A. Muñoz *et al.*, "Thermal stability of ARMCO iron processed by ECAP," *The Int. J. Adv. Manuf. Technol.*, vol. 98, pp. 2917–2932, 2018, doi: [10.1007/s00170-018-2353-7](https://doi.org/10.1007/s00170-018-2353-7).
- [27] S. Liu, D. Kent, H. Zhan, N. Doan, M. Dargush, and G. Wang, "Dynamic recrystallization of pure zinc during high strain-rate compression at ambient temperature," *Mater. Sci. Eng. A*, 784, no. 11, p. 139325, 2020, doi: [10.1016/j.msea.2020.139325](https://doi.org/10.1016/j.msea.2020.139325).